Nonlinear compressional waves in a two-dimensional Yukawa lattice

K. Avinash, P. Zhu, V. Nosenko, and J. Goree*
Department of Physics and Astronomy, The University of Iowa, Iowa City, Iowa 52242, USA
(Received 29 May 2003; published 8 October 2003)

A modified Korteweg–de Vries (KdV) equation is obtained for studying the propagation of nonlinear compressional waves and pulses in a chain of particles including the effect of damping. Suitably altering the linear phase velocity makes this equation useful also for the problem of phonon propagation in a two-dimensional (2D) lattice. Assuming a Yukawa potential, we use this method to model compressional wave propagation in a 2D plasma crystal, as in a recent experiment. By integrating the modified KdV equation the pulse is allowed to evolve, and good agreement with the experiment is found. It is shown that the speed of a compressional pulse increases with its amplitude, while the speed of a rarefactive pulse decreases. It is further discussed how the drag due to the background gas has a crucial role in weakening nonlinear effects and preventing the emergence of a soliton.

DOI: 10.1103/PhysRevE.68.046402 PACS number(s): 52.35.Mw, 63.22.+m, 82.70.Dd, 52.27.Lw

I. INTRODUCTION

Lattices with a reduced dimensionality are an interesting class of soft condensed matter. These lattices consist of particles which arrange themselves in a crystalline structure in the presence of external and interparticle forces. Typical examples of two-dimensional (2D) systems are colloidal suspensions [1], electrons on liquid helium [2], and Langmuir monolayers [3]. A number of interesting physical processes have been studied in these lattices, e.g., solid-liquid phase transitions, phonon propagation, and sublimation. Typical examples of 1D systems are quantum wires [4], one-dimensional surface states such as chains of H atoms on Ni(110) [5], O on Cu(110) [6], ion chains trapped in a storage ring [7], and optically bound chains of microspheres in a colloid [8].

Another way of preparing a lattice with reduced dimensionality is to use a plasma crystal, in which micron-size charged particles interact with each other via a Yukawa or screened-Coulomb potential. Most commonly, particles are levitated in a 2D lattice in the plasma sheath of a lower electrode, where an upward electric force balances gravity in the downward direction [9–12]. When the crystal anneals, a triangular lattice with hexagonal symmetry is formed. Experiments by Konopka *et al.* [13] and simulations by Schweigert *et al.* [14] have verified that in the plane of the 2D lattice, the interaction potential is modeled by a Yukawa potential. Hence, a 2D plasma crystal belongs to the general class of 2D Yukawa lattices. Similarly, 1D chains can be formed by shaping the particle suspension with a fence or a groove in an electrode [15].

For studying phonons or wave propagation, plasma crystals are ideal. Plasma crystals are suspended in a partially ionized, low-density plasma consisting of electrons, ions, and neutral gas. The particle motion is damped due to collisions with the neutral gas atoms. Since the background gas is much less dense than the fluid background in a colloidal suspension, the resulting damping rate is correspondingly smaller. This is conducive for the excitation and the propagation of lattice phonons.

Here, our work is motivated by experiments with linear and nonlinear waves launched in 2D plasma crystal. Nunomura *et al.* [16] used laser beams to launch linear longitudinal and transverse waves and measure their dispersion relations. They found an agreement with the theoretical dispersion relation of Wang *et al.* [17]. Samsonov *et al.* [18] launched a nonlinear pulse by applying a potential pulse to a wire located in the plane of the lattice. Nosenko *et al.* [19] launched nonlinear compressional pulses using a laser excitation technique. In the latter experiment, nonlinear effects were observed for large pulse amplitudes, as indicated by a pulse speed that increased with its amplitude. However, steepening of the pulse was not observed.

In this paper, we derive a modified Korteweg–de Vries (KdV) equation which is applicable to a wide class of interparticle potentials in 1D and 2D lattices. Starting with a chain of particles which interact with a potential of the class $U=U(|z_i-z_j|)$, where z_i is the position of the ith particle in the chain, a KdV-like equation is obtained under the continuum approximation. This can be applied to the problem of the propagation of nonlinear compressional waves in a 2D Yukawa lattice. Specifically, we show that the experimental geometry in a recent experiment [19] in a 2D plasma crystal allows us to model the pulse propagation by a suitably modified one-dimensional KdV equation. We take into account dispersion effects as well as damping due to the background gas.

We compare our results from solving the modified KdV equation with the experimental results of Nosenko *et al.* [19]. The agreement is found to be good. Our results underscore the crucial role of damping which weakens the nonlinear effects and prevents the emergence of solitons.

This paper is organized as follows. In Sec. II we derive a general KdV-like equation applicable to 1D. In Sec. III we explain how this equation can be applied to a 2D lattice. In Sec. IV we specialize to the case of 2D Yukawa lattice. In Sec. V we review some features of the inverse scattering transform theory that are relevant for our problem. In Sec. VI we apply this formalism to the case of plasma crystals and

*Electronic mail: john-goree@uiowa.edu

interpret the results of a recent experiment.

II. GENERAL FORMULATION

In this section we derive a general differential equation for the propagation of compressional nonlinear wave forms, such as nonlinear pulses and waves, in a 1D lattice. It can also be applied to a 2D lattice, as explained in Sec. III.

An equation for the compressional displacement of particles in a chain is obtained from the equation of motion using a Taylor expansion of the interparticle potential. Consider an infinite chain of particles which are separated uniformly by a distance a in the $\hat{z}$ direction. Let the interparticle potential between the ith and jth particles in the chain be given by $U_{ij}=U(|Z_i-Z_j|)$. The equation of motion of the jth particle is

$$m\frac{d^2Z_j}{dt^2}+m\nu_d\frac{dZ_j}{dt}=-\frac{\partial\sum_{j\neq i}U_{ij}}{\partial Z_j}+F_{ext}^j, \tag{1}$$

where m is the mass of the particle, ν_d is the coefficient of dissipation, and F_{ext}^j is the external perturbing force on the jth particle in the chain. We further assume that during the passage of the wave, the displacement η_j of the jth particle from its equilibrium position Z_{0j} in the chain is not very large. In this case, we expand $U(|Z_i-Z_j|)$ in powers of η_j/a and obtain the following difference equation for η_j [20]:

$$\begin{aligned}m\frac{d^2\eta_j}{dt^2}+m\nu_d\frac{d\eta_j}{dt}=-\Bigg\{&\Bigg[(\eta_{j-1}+\eta_{j+1}-2\eta_j)\frac{d^2U}{dZ^2}\Big|_a\\&+(\eta_{j-2}+\eta_{j+2}-2\eta_j)\frac{d^2U}{dZ^2}\Big|_{2a}+\cdots\Bigg]\\&+[(\eta_j-\eta_{j-1})^2-(\eta_{j+1}-\eta_j)^2]\frac{d^3U}{dZ^3}\Big|_a\\&+[(\eta_j-\eta_{j-2})^2-(\eta_{j+2}-\eta_j)^2]\frac{d^3U}{dZ^3}\Big|_{2a}\\&+\cdots\Bigg\}+F_{ext}^j.\end{aligned} \tag{2}$$

In Eq. (1) we have retained quadratic nonlinear terms.

If the typical scale length of the wave form L is greater than the interparticle distance a, then the continuum approximation can be invoked to convert the difference equation into a differential equation for η_j. Here, L can be the width of a pulse or the wavelength of a sinusoidal wave. We expand $\eta_{j\pm1}$ and $\eta_{j\pm2}$ around η_j in powers of a/L and retain terms of the order of $(a/L)^4$. In this approximation, nonlinear effects due to the particle discreteness are neglected. The expansions of $\eta_{j\pm1}$ and $\eta_{j\pm2}$ around η_j are given by

$$\eta_{j\pm1}=\eta_j\pm a\frac{\partial\eta_j}{\partial z}+\frac{a^2}{2}\frac{\partial^2\eta_j}{\partial z^2}\pm\frac{a^3}{3!}\frac{\partial^3\eta_j}{\partial z^3}+\frac{a^4}{4!}\frac{\partial^4\eta_j}{\partial z^4}, \tag{3}$$

$$\eta_{j\pm2}=\eta_j\pm2a\frac{\partial\eta_j}{\partial z}+\frac{(2a)^2}{2}\frac{\partial^2\eta_j}{\partial z^2}\pm\frac{(2a)^3}{3!}\frac{\partial^3\eta_j}{\partial z^3}+\frac{(2a)^4}{4!}\frac{\partial^4\eta_j}{\partial z^4}, \tag{4}$$

where the $\pm$ on the right-hand side (RHS) corresponds to the $\pm$ index on the left-hand side (LHS) of these equations. Substituting these expansions in Eq. (2) and retaining terms of the order of a^4, we obtain the following differential equation for the particle displacement η_j:

$$\frac{\partial^2\eta}{\partial t^2}+\nu_d\frac{\partial\eta}{\partial t}=v_p^2\frac{\partial^2\eta}{\partial z^2}+\frac{(v_p^2a^2)}{12}\frac{\partial^4\eta}{\partial z^4}-(2B)\frac{\partial\eta}{\partial z}\frac{\partial^2\eta}{\partial z^2}+\frac{F_{ext}}{m}, \tag{5}$$

where we have dropped the subscript from η and F_{ext}. In Eq. (5) the coefficients v_p and B are given by

$$v_p^2=a^2\left(\frac{d^2U}{dZ^2}\Big|_a+2^2\frac{d^2U}{dZ^2}\Big|_{2a}+3^2\frac{d^2U}{dZ^2}\Big|_{3a}+\cdots\right), \tag{6}$$

$$B=a^3\left(\frac{d^3U}{dZ^3}\Big|_a+2^3\frac{d^3U}{dZ^3}\Big|_{2a}+3^3\frac{d^3U}{dZ^3}\Big|_{3a}+\cdots\right). \tag{7}$$

The coefficient v_p in Eq. (5) is the linear phase velocity of longitudinal phonons in the chain.

An equation for the particle velocity $v=\partial\eta/\partial t$ is obtained by integrating Eq. (5) once with respect to time. If the nonlinearity is weak, the propagation speed of the wave form in the chain is expected to be close to v_p. In this case, a single integration with respect to time can be performed. We consider a case where the velocity of the pulse or other wave form is in the $-\hat{z}$ direction. This yields the following differential equation for v:

$$\frac{\partial v}{\partial t}+\nu_d v-v_p\frac{\partial v}{\partial z}-\frac{v_pa^2}{12}\frac{\partial^3v}{\partial z^3}+\frac{2B}{v_p^2}v\frac{\partial v}{\partial z}=\frac{F_{ext}}{m}. \tag{8}$$

This is a general initial-value problem for studying the temporal evolution of a initial wave form $v(z,0)$ excited by a transient perturbing force $F_{ext}(z,t)$ in a chain. For a given lattice potential U, the coefficients v_p and B in Eq. (8) can be calculated from Eqs. (6) and (7).

A variation of Eq. (8) which we found useful in Ref. [21] is suited for the time independent, steady-state excitation by F_{ext}. In a steady-state situation, the energy input of the drive due to a local perturbing force in the chain is balanced by the propagation and the dissipation of the wave energy away from the excitation region. This is a boundary-value problem. The corresponding equation for this case is obtained by

combining the terms containing $\partial v/\partial z$ in the RHS of Eq. (8) and transposing the coefficient to the LHS to give

$$\frac{v_p a^2}{12}\frac{\partial^3 v}{\partial z^3}+v_p\frac{\partial v}{\partial z}+\nu_d v=-\frac{\partial v}{\partial t}+\frac{2B}{v_p^2}v\frac{\partial v}{\partial t}. \tag{9}$$

This equation governs the steady-state propagation of wave forms in the chain. Here, the external perturbing force F_{ext} was dropped; its effect appears as a boundary condition on v in the excitation region. In the limit $L>a$, the sum in Eq. (1) converges rapidly and it is possible to integrate it numerically. However in this paper we do not choose this alternative, because by Taylor expanding the Yukawa potential we obtain a KdV-like equation which is easier to solve and, as we show later, gives reliable results.

III. APPLICATION OF THE 1D MODEL TO A 2D LATTICE

One of the chief points of this paper is that the model we have developed in the preceding section for a 1D chain can, in many cases, be applied to a 2D lattice. The procedure we used in Sec. II, expanding the interparticle potential yielding an equation for 1D, is by itself straightforward. What is less common is to extend this to a 2D problem. In this section, we summarize the conditions where this equation can be applied to a 2D lattice and we explain the critical step of substituting the phase velocity in this equation.

If a compressional wave in a 2D lattice has a straight-line wave front, it will propagate with a symmetry similar to the compressional wave in a 1D chain. In both cases, there is only one nontrivial coordinate, which we have denoted as z.

One difference between a 1D chain and a 2D lattice is that the latter is inherently anisotropic. For linear waves in a 2D lattice, the dispersion relation depends on the orientation of the lattice vector with respect to the wave number, especially for short wavelengths. However, this effect is negligible, provided that the wavelength is much longer than the interparticle spacing. By limiting our use of the model to long wavelengths, we avoid this difficulty. Doing so does not actually reduce the usefulness of our model, because in deriving our 1D equations we have already assumed that the wavelength is long compared to the particle spacing; we did this when we invoked the continuum approximation. If one wished to model a problem where our assumption of $L>a$ were not satisfied, then a different approach must be found that takes into account the anisotropy of a 2D lattice. One approach might be to use a multipole expansion. However, in the present problem, the assumption $L>a$ is satisfied and a simple approach based on a Taylor expansion of the interparticle potential is adequate.

The phase speed v_p is different in a 1D chain and a 2D lattice, and this must be taken into account. The reason for this difference is that in a triangular lattice, for example, interparticle bonds are oriented at three different angles, and bonds that are not perpendicular to the wave front are compressed less than those that are. Depending on the interparticle spacing, the phase speed in 2D can be higher or lower than in 1D.

The critical step that we have chosen for adjusting our model for the different phase speeds in a 1D chain and a 2D lattice is simply to substitute the phase speed v_p, as calculated for a 2D lattice into Eqs. (8) and (9). This is valid when conditions stated above are satisfied.

It is possible that this method can be extended to model planar waves in a 3D lattice as well, although we have not yet done so. What we have done, and we shall illustrate in the following section, is apply the 1D model to a 2D lattice with a Yukawa interparticle potential.

IV. APPLICATION TO A 2D YUKAWA LATTICE

In this section we apply the general formulation developed in the Sec. II for 1D chains to the specific case of a 2D Yukawa lattice at zero temperature.

The equation governing the propagation of a wave form in a Yukawa chain is obtained by substituting the expression for the Yukawa potential in Eqs. (6) and (7), and obtaining the coefficients of Eqs. (8) and (9). In a 1D Yukawa chain, charged particles repel one another with a screened-Coulomb potential of the form

$$U=\frac{Q^2}{4\pi\epsilon_0 Z_{ij}}\exp\left(-\frac{Z_{ij}}{\lambda}\right), \tag{10}$$

where $Z_{ij}=|Z_i-Z_j|$, Q is the particle charge, and λ is the screening scale length. Substituting Eq. (10) for U in Eqs. (6) and (7), we obtain

$$v_p^2=\frac{2Q^2}{ma}\left\{\kappa\left[1+\frac{e^\kappa(\kappa+2)-2}{2(e^\kappa-1)^2}\right]-\ln(e^\kappa-1)\right\}, \tag{11}$$

$$B=\frac{v_p^2 A}{2}, \tag{12}$$

where

$$A=\frac{\kappa^3+3\kappa^2+6\kappa+6}{\kappa^2+2\kappa+2} \tag{13}$$

and $\kappa\equiv a/\lambda$. In Eq. (11), the phase speed v_p is the speed of compressional phonons in the 1D Yukawa chain. With these expressions for the coefficients, Eqs. (8) and (9) become

$$\frac{\partial v}{\partial t}+\nu_d v-v_p\frac{\partial v}{\partial z}-\frac{v_p a^2}{12}\frac{\partial^3 v}{\partial z^3}-Av\frac{\partial v}{\partial z}=\frac{F_{ext}}{m} \tag{14}$$

and

$$\frac{v_p a^2}{12}\frac{\partial^3 v}{\partial z^3}+v_p\frac{\partial v}{\partial z}+\nu_d v=-\frac{\partial v}{\partial t}+Av\frac{\partial v}{\partial t}. \tag{15}$$

As in Eq. (8), we assume that the pulse or oscillatory wave is traveling in the $-\hat{z}$ direction. These equations are valid both for compressions and rarefactions, corresponding to v parallel and antiparallel to v_p, respectively. In Sec. VI we discuss the case of a rarefactive pulses.

As stated in the Sec. II, our method of using Eqs. (14) and (15) for a 1D Yukawa chain to model wave propagation in a 2D Yukawa lattice is to replace the phase velocity v_p by a different value appropriate for a 2D lattice. The reason for this is that the geometry of a 2D lattice is triangular rather than linear, hence the effective spring constant for the wave motion is different from the spring constant of a chain. As a consequence, the sound speed in a 2D lattice is different. Typically, it is greater than the 1D sound speed for small κ and smaller for large κ. Nunomura *et al.* [22] have calculated the sound speed v_{p2D} in a 2D Yukawa lattice at zero temperature for κ ranging from 0.1 to 10. For a 1D chain, the sound speed v_{p1D} can be obtained from Eq. (11) as a function of κ. From these, the ratio α of sound speeds in one and two dimensions is calculated as

$$\alpha \equiv \frac{v_{p2D}}{v_{p1D}}, \tag{16}$$

which depends on κ. Hence, to take into account the sound speed in a 2D triangular lattice when using our 1D model, we calculate v_p in Eq. (14) as

$$v_p^2 = \alpha^2 \frac{2Q^2}{ma}\left\{\kappa\left[1+\frac{e^\kappa(\kappa+2)-2}{2(e^\kappa-1)^2}\right]-\ln(e^\kappa-1)\right\}. \tag{17}$$

Thus, the propagation of a compressional wave form in a 2D Yukawa lattice, having a nearly straight-line wave front, can be studied via Eq. (14) with the coefficients v_p and A given by Eq. (17) and Eq. (13), respectively. The ratio α in Eq. (17) must be calculated from Eq. (16) using values, for example, from Ref. [22] for v_{p2D} at a given value of κ.

V. INVERSE SCATTERING TRANSFORM METHOD

Without the term corresponding to the external force F_{ext}, Eq. (14) belongs to the general class of KdV equations which are solved by the method of inverse scattering transform (IST). Here, we review the relevant features of this method [23], given as follows.

(1) The KdV equation is

$$\frac{\partial v}{\partial t}+\mu\frac{\partial v}{\partial z}+\nu v\frac{\partial v}{\partial z}+\gamma\frac{\partial^3 v}{\partial z^3}=0, \tag{18}$$

where μ, ν, and γ are constants. It has a unique solution for all those classes of initial conditions $v(z,0)$ which vanish rapidly as $z\to\infty$.

(2) The information about the number of solitons and their respective velocities is obtained by solving the corresponding Schrodinger equation with $v(z,0)$ as the potential:

$$\frac{d^2v}{dz^2}-[v(z,0)-\lambda_N]v=0. \tag{19}$$

For every $v(z,0)$ satisfying Eq. (19), there exists a finite set of discrete eigenvalues λ_N where $N=1,2,3,\ldots$. In addition, there may be a continuous spectrum of eigenvalues.

The general solution of the KdV equation consists of terms corresponding to the soliton and the dispersion. For an initial pulse $v(z,0)$ this solution is given by

$$v(z,t)=v_N(z,t)+O(\sigma(t)), \tag{20}$$

where $v_N(z,t)$ is the N-soliton solution and the last term corresponds to dispersion. This solution can be constructed from the scattering data, which must be obtained by solving Eq. (19) for a given initial pulse $v(z,0)$. Once the scattering data are available, then $v_N(z,t)$ can be constructed following the procedure outlined in the IST theory [23]. The velocity of the Nth soliton is proportional to the λ_N. The second term of the solution in Eq. (20) is the dispersive part due to the continuous spectrum of the eigenvalues. Under very general conditions, it phase mixes to zero as $t\to\infty$. It should be noted that IST is a complete theory which describes much more than what we have stated here briefly. An estimate of the number of solitons for a given initial pulse $v(z,0)$ is given by

$$N\leqslant 2+\int |z||v(z,0)|dz. \tag{21}$$

Clearly, an initial pulse with a larger amplitude allows the generation of more solitons. Interestingly, there is an exact solution for two solitons given by

$$v_2(z,t) = -12\left\{\frac{[3+4\cosh(2z-8v_pt)+\cosh(4z-64v_pt)]}{[3\cosh(z-28v_pt)+\cosh(3z-36v_pt)]^2}\right\}. \tag{22}$$

The measurement of the shape of the initial pulse is of prime importance in the transient excitation experiments. This is for two reasons. First, the shape of the initial wave form is required in the initial-value problem. Second, according to the IST theory outlined above, if the conditions are appropriate then an N-soliton solution will emerge from the initial pulse as $t\to\infty$. All the information about the soliton solution, including the number of solitons and their speeds, is contained in the initial pulse $v(z,0)$.

VI. NONLINEAR PULSES IN PLASMA CRYSTALS

In this section, we apply the general formulation developed earlier to the specific case of the excitation of transient pulses in plasma crystals. We then interpret the results of recent experiments.

A. Modeling the initial-value problem

The solution of the initial-value problem in Eq. (14) is useful for modeling experiments with the transient excitation of a compressional pulse in a plasma crystal. In the experiment of Nosenko *et al.* [19], a compressional pulse was launched in a 2D plasma crystal by the radiation pressure force of a laser sheet which was momentarily turned on and then off. This resulted in a weakly nonlinear pulse, where the

perturbed particle velocities were all in one direction and the resulting wave front was nearly a straight line. Hence, for reasons given earlier, the propagation of this nonlinear pulse can be approximated by the propagation of a pulse along a linear Yukawa chain. In the experiment, the pulse shape along the direction of propagation was measured at the initial time as well as at subsequent intervals. The solution of the initial-value problem in Eq. (14) with v_p given by Eq. (17) is thus applicable. If we take the shape of the pulse after the laser was turned off, we may simplify Eq. (14) by dropping the F_{ext} term. Hence, we will solve Eq. (14) without F_{ext}, and use as its initial condition the pulse shape just after the laser was turned off.

In the case of a plasma crystal, we identify the screening scale length λ in Eq. (10) as the Debye length λ_D. In the plasma crystal, the particle charge is screened by the background electrons and ions. Hence, the screening scale length is given by the Debye length in the expression for the Yukawa potential.

Before proceeding to construct the solution, we next discuss the crucial effects of dissipation in our solutions.

B. Damping

Any possible source of damping in the experiment reduces the pulse's amplitude and weakens any nonlinear effects. In the experiment, a plasma crystal is formed in a rf plasma which has not only electrons and ions but also neutral molecules of the background gas. The collisions of the dust particles with gas molecules give rise to a damping of the particle motion. Using Epstein's model, the coefficient of this drag ν_d in Eq. (14) is given by [22]

$$\nu_d = \delta \sqrt{\frac{8m_g}{\pi T_g}} \frac{p}{\rho r_p}, \tag{23}$$

where p, m_g, T_g, r_p, and ρ are the gas pressure, mass of the gas molecule, gas temperature, radius, and the material density of particles, respectively. The leading coefficient δ ranges from 1.00 in the case of the specular reflection to 1.44 in the case of diffuse reflection. Typical values of ν_d for micron-size particles in about 10-mtorr gas are of the order of 1 s^{-1}. In the experiment by Nosenko *et al.* [19], $\nu_d = 2.9\ s^{-1}$.

The role of damping becomes even more crucial in experiments where the amplitude of the initial pulse is not very large. As we shall see shortly in our solutions, the damping quickly reduces the amplitude of the initial pulse. Hence, the main effect of the damping is to weaken nonlinear effects before a well-defined soliton may emerge. Earlier, Rosenberg and Kalman [24] found that damping can similarly obscure the effects of correlations in the dispersion of acoustic waves in a 3D dusty plasma.

C. Evolution of the pulse

In the experiment, a pulse was excited by applying the radiation pressure force due to a laser sheet. The laser sheet struck the lattice at an angle, applying a force in the $-\hat{z}$ direction within a narrow excitation region. Thereafter, a compressional pulse propagated in the $-\hat{z}$ direction. A larger laser power resulted in larger amplitude pulses in the lattice. Particle positions, recorded by a video camera, were used to calculate the particle velocity and the areal number density as the pulse propagated through the lattice. Depending on the number of particles, the interparticle distance a ranged from 486 μm to 1097 μm and the values of κ ranged from 0.68 to 1.45. In Fig. 1 we show the experimental data for the pulse shape from Ref. [19]. The initial pulse is identified as curve 0, which was recorded just after the laser was turned off. Its subsequent evolution at intervals of 0.1 s up to 0.5 s are also shown. The laser power was 2.38 W.

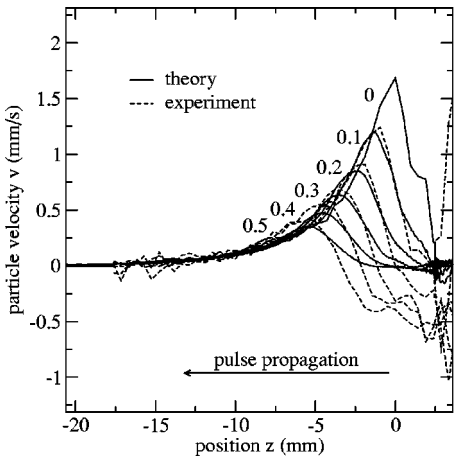

FIG. 1. Propagation of a compressional pulse in a 2D lattice. Parameters used in the theory were $\kappa = 1.45$, $a = 1.05$ mm, $v_p = 9$ mm/s, and $\nu_d = 2.9\ s^{-1}$. The experimental curve at $t = 0$ was recorded after the laser was turned off; it was used as the initial condition for the theory. The pulse shape is also shown at five subsequent intervals of 0.1 s. The theoretical curves are superimposed on the experimental observations of Nosenko *et al.* [19].

The experimental parameters had uncertainties that must be taken into account while explaining the observations. The temporal evolution of the initial pulse $v(z,0)$ is studied by solving Eq. (14). If parameters such as the particle charge Q, mass m, and κ which enter in the coefficients of various terms in Eq. (14) were known with infinite precision, then there would be no free parameters in the problem and the evolution of the initial pulse $v(z,0)$ would be unique. However, because of the inevitable experimental errors in the measurement of these parameters, there is a range of values of the coefficients in Eq. (14) to choose from. In the experiment, the charge was $Q = -(9000 \pm 200)e$, the particle diameter was $D = 8.09 \pm 0.18$ μm, and the error in the measurement of κ, which was made using a wave technique, was $\Delta\kappa/\kappa = \pm\ 0.13$. The parameter known with the greatest precision in the experiment was a [19].

The error in v_p, denoted by Δv_p, arises mainly due to errors in measurements of Q, D, and κ. Using the method of propagation of errors, we obtain $\Delta v_p / v_p$ as

$$\frac{\Delta v_p}{v_p} = \pm \sqrt{\left[\left(\frac{\Delta Q}{Q}\right)^2 + \left(\frac{3\Delta D}{2D}\right)^2 + \left(\frac{\Delta\kappa}{2f}\frac{df}{d\kappa}\right)^2\right]}, \tag{24}$$

where $f(\kappa)$ is the κ dependence of v_p^2 given in Eq. (17).

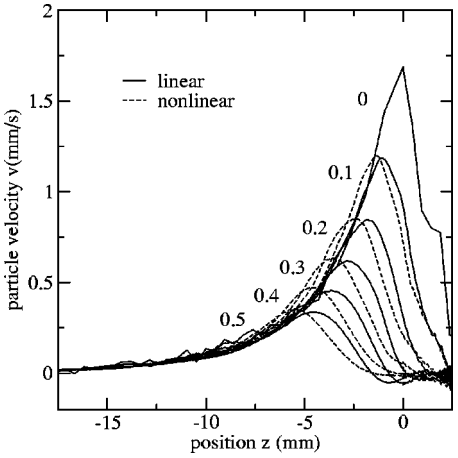

FIG. 2. The evolution of the initial pulse with and without the nonlinear term in Eq. (14). This test demonstrates that for conditions as in the experiment ($\kappa=1.45$, $a=1.05$ mm, $v_p=9$ mm/s, and $\nu_d=2.9\ \mathrm{s}^{-1}$), nonlinearities affect the pulse's speed but not its shape. The pulse shape is shown at five subsequent intervals of 0.1 s.

Using the experimental uncertainties for Q, D, and κ, we obtain $v_p=29\pm3$ mm/s for $\kappa=0.68\pm0.09$ and $a=0.50$ mm, and $v_p=10.00\pm1.00$ mm/s for $\kappa=1.45\pm0.18$ and $a=1.05$ mm. The particle's mass density in both cases is 1.514 g/cm^3. Our results for the uncertainties of v_p, given above, correspond to a 1-σ range. It is within this range that we will constrain v_p, when fitting our model to the experimental data.

We solve Eq. (14), using as its initial condition the experimental pulse shape identified as curve 0 in Fig. 1. We also show the temporal evolution of this pulse at subsequent intervals of 0.1 s. For the best fit to the experimental results, we have chosen $a=1.05$ mm, $\kappa=1.45$, $A(\kappa)=3.43$; we also chose $v_p=9$ mm/s, which is at the lower end of the 1-σ range given above. As stated earlier, the shape of the pulse after the laser is turned off is required as the initial condition in Eq. (14). Because Eq. (14) is written for a pulse moving in the $-\hat{z}$ direction, we replace the portion of the experimental wave form at $z>2.5$ mm, which contained a rarefactive pulse moving in the $+\hat{z}$ direction, with a zero value. The compression portion of the experimental wave form, $z<2.5$ mm, is retained. We then evolve the pulse shape as it propagates by integrating Eq. (14). For easy comparison with the experiment we rescale our equation in physical units: distance in millimeters, time in seconds, and the speed in mm/s. As in the experiment, the evolution of the pulse is obtained at time intervals of 0.1 s up to 0.5 s. This is shown in Fig. 1. The agreement of the solutions with experimental results is good.

As stated earlier, damping reduces the role of nonlinear effects. Because of damping, the amplitude decays and the nonlinearity is weakened. As a result, in the late stages of the pulse's evolution, its shape is governed mostly by linear terms. To demonstrate this, in Fig. 2 we show the evolution of the initial pulse in Fig. 1 as calculated both with and without the nonlinear term in Eq. (14). This comparison shows that except for the higher speed of the pulse with the nonlinear term, the difference is not very significant.

The condition for the emergence of a soliton from the initial pulse requires that the nonlinear term must persist indefinitely despite damping. In Fig. 1 we see that the solution has developed a significant oscillatory part that is not yet damped. This part corresponds to the second term of Eq. (21). The dispersive part will decay to zero as $t\rightarrow\infty$. Thus, the condition for the emergence of a soliton is that the nonlinear terms persist for a time long enough for the oscillatory part to damp to a low level. This requires either (a) a sufficiently large amplitude of the initial pulse or (b) a small damping rate. In the experiment of Nosenko *et al.* [19], the pulse amplitude was rather weak, $v<1.8$ mm/s, so that nonlinear effects were not strong, and these were further weakened by the damping at a rate $\nu_d\approx2.9\ \mathrm{s}^{-1}$. This explains why a clear soliton did not emerge from the initial pulse in this experiment.

If an experiment had an initial pulse with a much larger amplitude, there might be not only one but several solitons. As discussed earlier, the initial pulse corresponds to a potential in the Schrödinger equation. The depth of the well is proportional to the amplitude of the pulse. Since a deeper potential well accommodates more eigenvalues, and since the number of eigenvalues is equal to the number of solitons, it follows that the number of solitons emerging from an initial pulse increases with its amplitude. This is also consistent with the estimate of number of solitons given by Eq. (22).

D. Speed of the pulse

The speed of a nonlinear pulse is in general a function of its amplitude. This was observed to occur in the experiment of Ref. [19]. The experimenters found that the increase in speed, as compared to the linear case, was roughly proportional to the amplitude. This nonlinear effect was observed most strongly at large κ. The experiment was performed for laser powers of 0.66 W, 1.25 W, 1.84 W, 2.38 W, and 2.75 W, where higher laser powers yielded larger amplitudes for the pulse.

For both the experiment and the theory, our method of measuring the speed of the pulse was to plot its position z_0 vs t and fit it to a straight line. The method of identifying z_0, however, was different for the theory where we could easily identify the maximum of the pulse's peak, and the experiment where we could not, due to noise in the data. The position of the peak in the experiment was determined in two steps. First, z_0 was estimated by the point z_{max} where the particle velocity is maximum. Second, to reduce the effect of noise, the first moment of v vs z was calculated using data in the range $z_{max}-2.5$ mm to $z_{max}+2.5$ mm.

We evolved the pulses by solving Eq. (14) and we obtained the pulse speed V as a function of the amplitude. We repeated this calculation for amplitudes corresponding to each of the five values of laser power in the experiment: 0.66 W, 1.25 W, 1.84 W, 2.38 W, and 2.75 W. We also repeated it for two values of κ: 0.68 and 1.45. We then compare the pulse speeds from the experiment and the theory. For $\kappa=1.45$, in the theory we used the value of v_p discussed

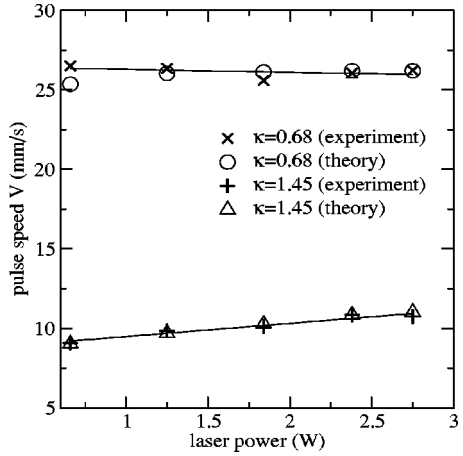

FIG. 3. Variation of pulse speed V with amplitude. In the experiment, the amplitude increased with the applied laser power. In the theory, the amplitude for the initial condition was chosen to match the experiment, and the parameters $v_p = 26$ mm/s for $\kappa = 0.68$ and $v_p = 9$ mm/s for $\kappa = 1.45$ were assumed. The value of ν_d was same as in Fig. 1. For large κ, the pulse speed increases significantly with amplitude. Experimental data are fitted to a straight line.

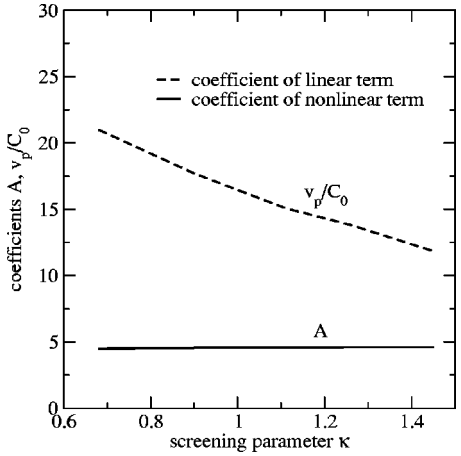

FIG. 4. The coefficients v_p/C_0 and A of the linear and nonlinear terms, respectively in Eq. (14), as a function of κ. Here, $C_0 = Q/\sqrt{ma}$. For small κ the coefficient of the linear term is much larger than that of the nonlinear term. This results in a linear behavior at small values of κ.

earlier. For $\kappa = 0.68$, we chose $v_p = 26$ mm/s for a good fit; this value is again at the lower end of the 1-σ range from the experiment. In Fig. 3 we show results for pulse speed vs amplitude both in theory and experiment, and we note that the agreement is good.

The reason that the pulse speed is independent of the amplitude for small values of κ is that v_p varies rapidly with κ. Recall that the phase velocity v_p that appears as the coefficient of the linear term in Eq. (14) is given by Eq. (11). This velocity increases rapidly with decreasing κ. On the other hand, the parameter $A(\kappa)$, which is the coefficient of the nonlinear term in the same equation, varies slowly with κ. These two variations are shown in Fig. 4. Thus, with decreasing κ, linear terms become more dominant than the nonlinear terms, leading to a linear behavior at small values of κ.

We can justify now the experimenters' choice of fitting their data for pulse speed vs amplitude to a straight line [19]. Their idea for choosing a straight line rather than some other power law came from the theory for a nonlinear adiabatic sound wave in a 3D fluid [25]. They chose this form, despite the difference of their 2D crystal and a 3D fluid, for a lack of any better model. Here, we present a justification based on our model, for fitting pulse speed vs amplitude to a straight line, for 1D propagation in a 2D lattice. As shown by Nosenko *et al.* [19], the role of dispersion in the pulse propagation is weak. In this case we may neglect the dispersion term in Eq. (14) and express it as

$$\frac{\partial v}{\partial t} + \nu_d v = v_p \left(1 + A\frac{v}{v_p}\right)\frac{\partial v}{\partial z}. \tag{25}$$

In the experiment the nonlinearity is weak, i.e., $v/v_p \ll 1$. For such a case Eq. (25) corresponds to a pulse with a speed

$$|V| = v_p + Av, \tag{26}$$

where v and v_p are positive values.

Finally, we discuss rarefactive pulses, which we find have a speed that decreases with their amplitude. In the initial condition for a rarefactive pulse, the particle velocity is in the direction opposite to the pulse propagation velocity. Since in Eq. (14), the pulse propagation was assumed to be in $-\hat{z}$ direction, then v in the initial condition for a rarefactive pulse should be in the $+\hat{z}$ direction.

For example, an initial condition for a rarefactive pulse in Eq. (14) can be obtained by assuming an initial pulse such as that in Fig. 1 but with v in the opposite direction. To demonstrate this, as an initial condition for a rarefactive pulse we reversed the sign of v for curve 0 in Fig. 1, retaining the

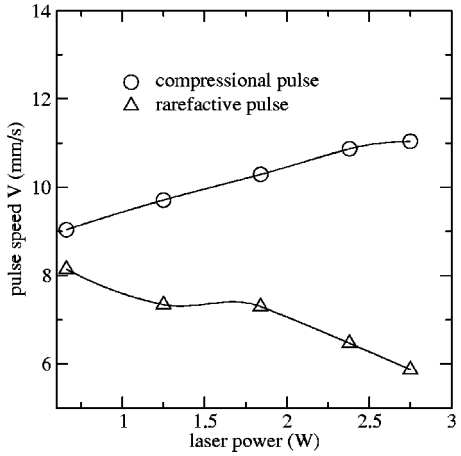

FIG. 5. Variation of the pulse speed with the amplitude for compressional and rarefactive pulses. Data shown are from theory. Parameters assumed were the same as in Fig. 1. The pulse amplitude in the theory was chosen to match the compressional pulse amplitude in the experiment at various laser powers. A smooth curve is drawn through the data points.

initial data for $z<2.5$ mm, as before. This pulse was then evolved by solving Eq. (14), and the speed vs amplitude relationship was obtained as before. In Fig. 5 we show the results for both compressional and rarefactive pulses, assuming $\kappa=1.45$, $a=1.05$ mm, and $v_p=9$ mm/s. We find that, as opposed to the case of the compressional pulse, the speed of the rarefactive pulse is found to decrease with the amplitude, as shown in Fig. 5.

VII. SUMMARY

In this paper we have developed a general formalism to study the propagation of nonlinear wave forms, such as nonlinear pulses and waves, in 1D chains and 2D lattices. By Taylor expanding the interparticle potential in the equation of motion, an equation governing the propagation of transient or steady-state wave forms in a 1D chain is obtained.

By suitably changing the linear phase velocity in the 1D equation and assuming a Yukawa potential between particles in the chain, this formalism was applied to the case of a 2D plasma crystal. The initial-value problem in Eq. (14) was demonstrated using the experimentally measured $v(z,0)$ as the initial condition. We accounted for the damping due to the background neutral gas. The calculated evolution agrees well with the experimental observations of Nosenko *et al.* [19]. The speed of the compressional pulse was shown to increase with its amplitude, which is consistent with the experimental observations. The speed of rarefactive pulse is shown to decrease with the amplitude.

We discuss how damping plays a crucial role in weakening nonlinear effects in the experiment of Nosenko *et al.* [19]. In this experiment the amplitude of the initial pulse was not very large. The drag due to neutrals further weakens the nonlinearity quickly by damping the pulse's amplitude. As a result, the emergence of a soliton is prevented and in the late stages of the pulse's evolution its propagation is governed mostly by linear effects.

ACKNOWLEDGMENTS

We thank A. Bhattacharjee for useful discussions. This work was supported by NASA and the U.S. Department of Energy.

[1] V.M. Kaganer, H. Mohwald, and P. Dutta, Rev. Mod. Phys. **71**, 779 (1999).
[2] F.M. Peeters and X. Wu, Phys. Rev. A **35**, 3109 (1987).
[3] C.C. Grimes and G. Adams, Phys. Rev. Lett. **42**, 795 (1979).
[4] A. Yacoby *et al.*, Phys. Rev. Lett. **77**, 4612 (1996).
[5] U. Bischler and E. Bertel, Phys. Rev. Lett. **71**, 2296 (1993).
[6] E. Bertel and J. Lehmann, Phys. Rev. Lett. **80**, 1497 (1998).
[7] J. Pachos and H. Walther, Phys. Rev. Lett. **89**, 187903 (2002).
[8] S.A. Tatarkova, A.E. Carruthers, and K. Dholakia, Phys. Rev. Lett. **89**, 283901 (2002).
[9] J.H. Chu and L. I, Phys. Rev. Lett. **72**, 4009 (1994).
[10] H. Thomas, G.E. Morfill, V. Demmel, J. Goree, B. Feuerbacher, and D. Möhlmann, Phys. Rev. Lett. **73**, 652 (1994).
[11] Y. Hayashi and K. Tachibana, Jpn. J. Appl. Phys., Part 2 **33**, L804 (1994).
[12] A. Melzer, T. Trottenberg, and A. Piel, Phys. Lett. A **191**, 301 (1994).
[13] U. Konopka, G.E. Morfill, and L. Ratke, Phys. Rev. Lett. **84**, 891 (2000).
[14] I.V. Schweigert, V.A. Schweigert, A. Melzer and A. Piel, Phys. Rev. E **62**, 1238 (2000).
[15] A. Homann, A. Melzer, S. Peters, and A. Piel, Phys. Rev. E **56**, 7138 (1997).
[16] S. Nunomura, J. Goree, S. Hu, X. Wang, A. Bhattacharjee, and K. Avinash, Phys. Rev. Lett. **89**, 035001 (2002).
[17] X. Wang, A. Bhattacharjee, and S. Hu, Phys. Rev. Lett. **86**, 2569 (2001).
[18] D. Samsonov, A.V. Ivlev, R.A. Quinn, G. Morfill, and S. Zhdanov, Phys. Rev. Lett. **88**, 095004 (2002).
[19] V. Nosenko, S. Nunomura, and J. Goree, Phys. Rev. Lett. **88**, 215002 (2002).
[20] F. Melandsø, Phys. Plasmas **3**, 3809 (1996).
[21] V. Nosenko, K. Avinash, J. Goree, and B. Liu, Phys. Rev. Lett (to be published).
[22] S. Nunomura, J. Goree, S. Hu, X. Wang, and A. Bhattacharjee, Phys. Rev. E **65**, 066402 (2002).
[23] V. Eckhaus and A. Van Harten, *The Inverse Scattering Transform and the Theory of Solitons, An Introduction* (North-Holland, New York, 1981).
[24] M. Rosenberg and G. Kalman, Phys. Rev. E **56**, 7166 (1997).
[25] L.D. Landau and E.M. Lifshitz, *Fluid Mechanics* (Butterworth-Heinemann, Boston, 1997), Vol. 6.